

## Photon Emission STM Using Optical Fiber Bunches

C. Thirstrup<sup>a,b)</sup>, M. Sakurai<sup>a)</sup>, and M. Aono<sup>a,c)</sup>

*a) The Institute of Physical and Chemical Research (RIKEN), Wako, Saitama 351-01, Japan*

*b) Core Research for Evolutional Science and Technology (CREST) Program, Japan Science and Technology Corporation (JST), Japan*

*c) Department of Precision Science and Technology, Osaka University, Suita, Osaka 565, Japan*

(Received: 15 March 1998; accepted: 25 March 1998)

### Abstract

A photon emission scanning tunneling microscope (PE-STM) operating in ultra high vacuum (UHV) and comprising an optical fiber bunch is reported. The optical fiber bunch is readily positioned close to the tip-sample region of the STM using an xyz-manipulator to obtain a good collection efficiency of the photons (with the present system ~4.5 %, but this can be improved using fibers with a higher numerical aperture). The system exhibits a low number of undesirable photon counts from the stainless steel walls and the ion pump in the UHV chamber. Examples of spatial distributions of photon emission (photon maps) are presented from gold surfaces with a quantum efficiency of the photon emission process (QE) of  $10^{-3}$  and from exposed dangling bonds on silicon (001) surfaces terminated by deuterium with a QE of  $10^{-6}$ . Even for the case of low QE, good contrasts with atomic resolution can be obtained in the photon maps.

### 1. Introduction

Gimzewski et al.<sup>1</sup> and Berndt et al.<sup>2-4</sup> have shown using a scanning tunneling microscope (STM) that photon emission characteristics can be obtained from areas with nanometer and molecular resolution yielding important information about surfaces or individual molecules. Various ways have been utilized to detect photons emitted from the tunnel junction of an STM tip including placing a detector close to the tip-sample region<sup>1,5</sup>, using a lens<sup>3,6-8</sup>, a prism coupler<sup>9</sup> or a plastic fiber<sup>10</sup> to collect the photons. Also a conductive transparent tip has been used to collect photons<sup>11</sup>. When recording the spatial distribution of the photon emission (photon maps) from atomic scale structures, one usually has to operate at low photon count numbers, in many cases close to the dark count level. There are several reasons for this. The photon map requires a large number of measurement points, typically 128x128 pixels, and a reasonable time to record the data is  $\leq 30$ min implying that the measuring time at each pixel ( $t_{\text{pixel}}$ ) is  $< 100$  ms. In order to achieve atomic resolution and avoid desorption of atoms from the surface, it is limited how large tunnel currents and voltages that can be used to achieve an acceptable photon count number. The physical geometries of a UHV-STM also restrict the number of photons that can be collected. Usually, this number is a few percent of the photons emitted from the STM tip in a solid angle of  $4\pi$ .

The authors of the present paper have previously reported the mechanism of photon emission from dangling bonds on Si(001) hydrogen terminated surfaces<sup>12</sup>. Here we focus on the measuring system comprising a UHV photon emission STM (PE-STM) where the collection of photons is based on an optical fiber bunch mounted inside the UHV chamber. Examples of photon maps recorded using this system will be presented. The diameter of the fiber bunch is 1 mm and the numerical aperture of each fiber (N.A.) is 0.56. The overall collection efficiency ( $\eta$ ) of the system is ~4.5%, but using fibers with a higher N.A., it is possible to increase  $\eta$ . For the purpose of collecting photons from an STM tip, optical fiber bunches have the advantage compared to lenses that the number of undesirable photons collected from stainless steel walls and ion-pumps in the UHV chamber can easily be minimized.

Using the system, photon emission was investigated for n-type and p-type deuterium (D) terminated Si(001) (3x1) reconstructed surfaces [Si(001)-(3x1)-D surfaces] and a gold (Au) film evaporated onto the native oxide of a Si(001) sample. The latter type of sample was used as a reference, since the quantum efficiency (QE) of the photon emission from Au surfaces is high<sup>13</sup> ( $\sim 10^{-3}$ ) and Au surfaces have been studied extensively by many research groups<sup>2,4,5,9,10,14,15</sup>. On the other hand, the QE of the photon emission from Si(001) surfaces is much lower ( $\sim 10^{-6}$ )

and has only been studied by one other research group as far as it is within the authors' knowledge. In this case, tunnel currents of several hundreds nA and voltages of several tens of volts were employed<sup>6</sup>. In the experiments presented in the present paper, the bias voltages were of the order of 3 V and the tunnel currents were in the range 2-8 nA. At these operating conditions, photon maps on the atomic scale could be recorded.

## 2. Experimental Setup and Sample Preparation

A schematic of the experimental setup is depicted in Fig. 1. A commercial JEOL STM (JSTM-4000XV) operating at room temperature in a UHV-chamber with a base pressure of  $\sim 8 \times 10^{-9}$  Pa was employed. The photons emitted from the tip of the STM were collected by an optical fiber bunch. The fibers supplied by Hoya Schott and exhibiting constant optical transmission from 400 to 1100 nm were assembled in stainless steel tubes, glued using vacuum seal, cured at 100°C and each end of the fiber bunch was polished using various types of sand papers, the finest one with a grain size of  $0.5 \mu\text{m}$ . The fiber bunch was mounted in the UHV chamber. The input end of the fiber bunch was positioned close to the tip-sample region of the PE-STM using an

xyz-translation stage from Vacuum Generators (see Fig. 2 which is a photograph of the system focussing on the part including the STM tip, the sample and the optical fiber bunch). The output end of the fiber bunch was mounted close to a quartz viewport, and an antireflect-coated  $f/0.7$  lens positioned outside the UHV-chamber imaged the output end of the fiber bunch onto a Hamamatsu R2949 cooled photomultiplier tube (PMT) [see Fig. 1] operating in photon counting mode. The fiber bunch holder mounted close to the viewport also acted as a shield against undesirable photon counts from the stainless steel walls and the ion-pump in the UHV chamber.

The distance in Fig.2 between the tip apex and the fiber bunch is  $\sim 700 \mu\text{m}$  and the angle ( $\theta$ ) between the surface normal and the fiber bunch axis is  $56^\circ$ . It is possible to position the fiber bunch closer to the tip apex or decrease  $\theta$ , but nothing is achieved in terms of collection efficiency since it is determined by the N.A. of the fiber bunch. With the present system, the overall photon collection efficiency ( $\eta$ ) was estimated to be  $\sim 4.5\%$ . Using a larger N.A. of for example 0.72, which is commercially available,  $\eta$  is estimated to be increased to  $\sim 8\%$ . In this case, the end of the fiber bunch with a diameter of 1 mm should be positioned

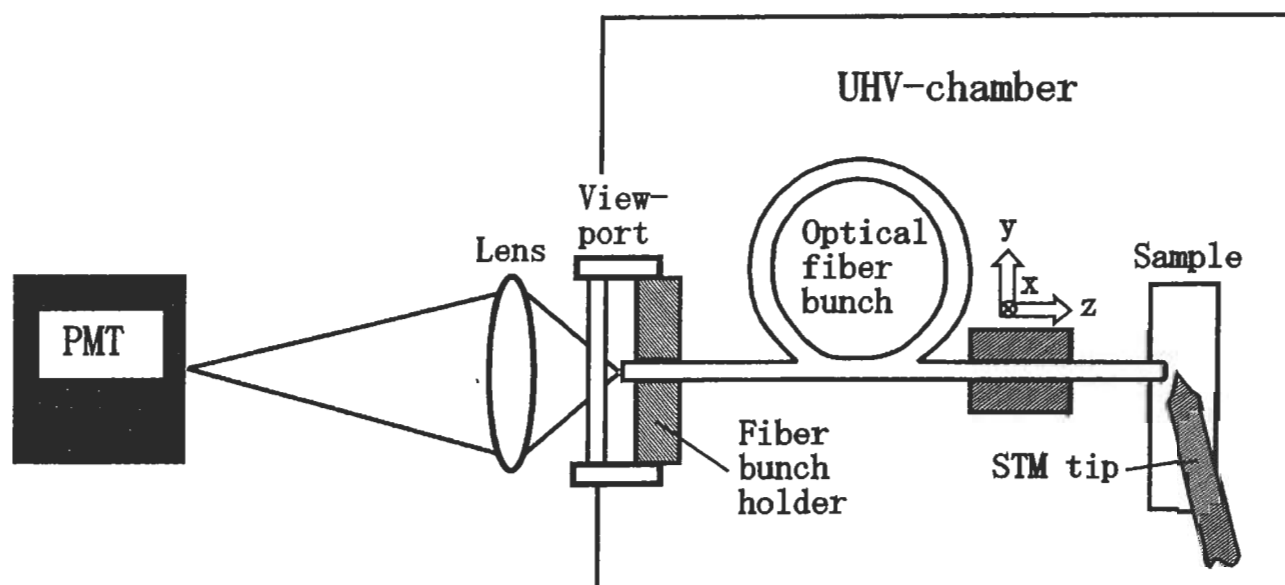


Fig.1 Experimental setup of the photon emission scanning tunneling microscope (PE-STM) employing an optical fiber bunch to collect the photons emitted from the STM tip. The STM and the optical fiber bunch is mounted inside an ultra high vacuum (UHV) chamber. The input end of the fiber bunch is positioned close to the tip-sample region using an xyz-manipulator. The output end is mounted close to a viewport by means of a holder which also acts as a shield against undesirable photon counts from the stainless steel walls and the ion-pump in the UHV chamber. A lens mounted outside the UHV chamber images the output end of the optical fiber bunch onto a photomultiplier tube (PMT).

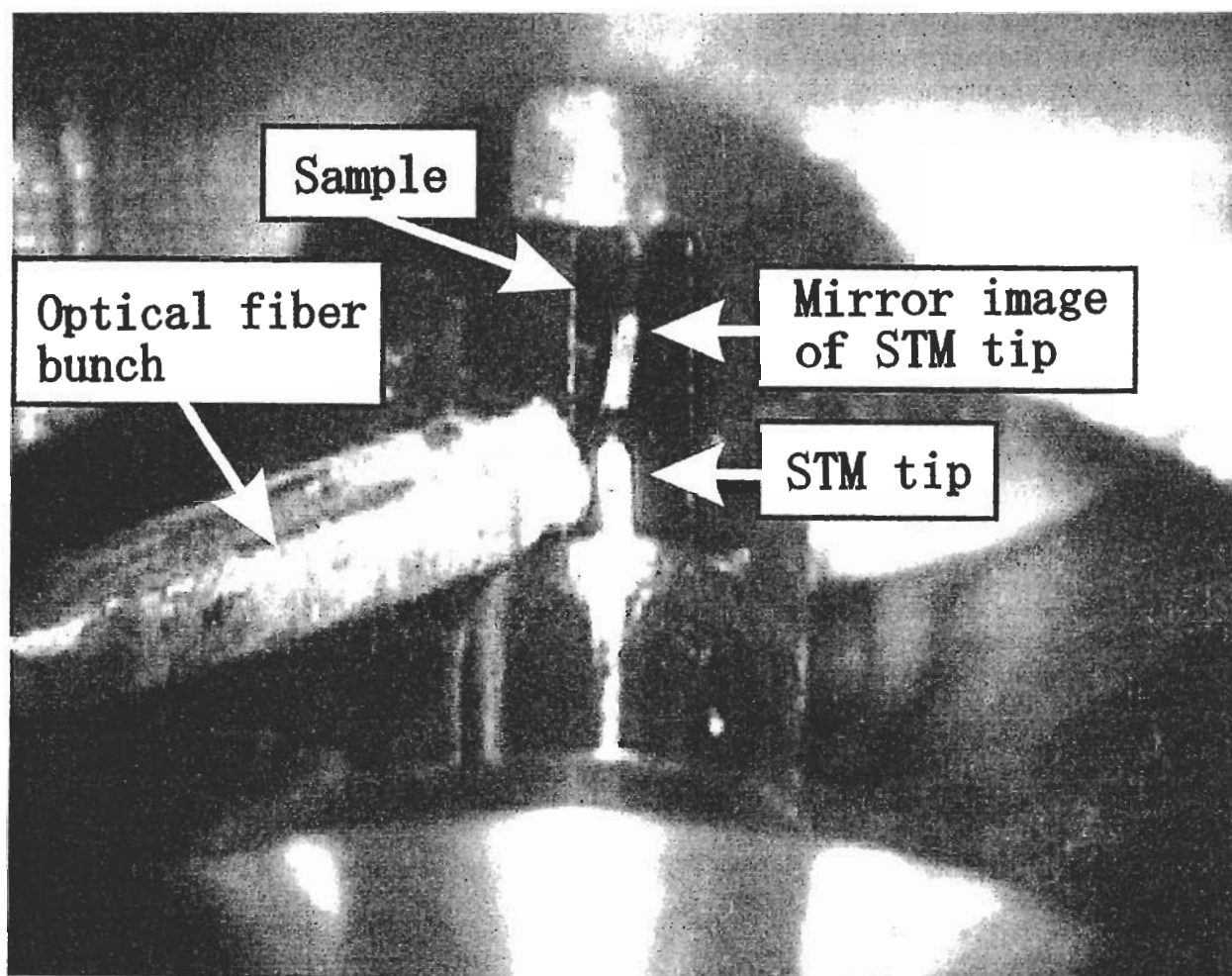


Fig.2 Photograph of the PE-STM focussing on the part including the STM tip, the sample and the optical fiber bunch.

500  $\mu$  m from the STM tip apex with  $\theta = 45^\circ$ . With such a small distance between the end of the fiber bunch and the tip apex, the diameter of the STM tip then needs to be reduced accordingly. Another way to increase  $\eta$  is of course to mount two or more fiber bunches in the chamber. Since optical fiber bunches only collect photons from a small area near the tip-sample region, the number of undesirable photons collected from the stainless steel walls and the ion-pump in the UHV chamber is low. The ion-pump was kept turned on during the photon emission experiments. Turning it off did not make any noticeable change in the dark count rate of the PMT ( $\sim 10$  CPS).

The photons were counted using a Stanford for Research SR 400 photon counter connected to a PC. A trigger circuit enabled photon maps to be recorded quasi-simultaneously with constant tunnel current topographs.

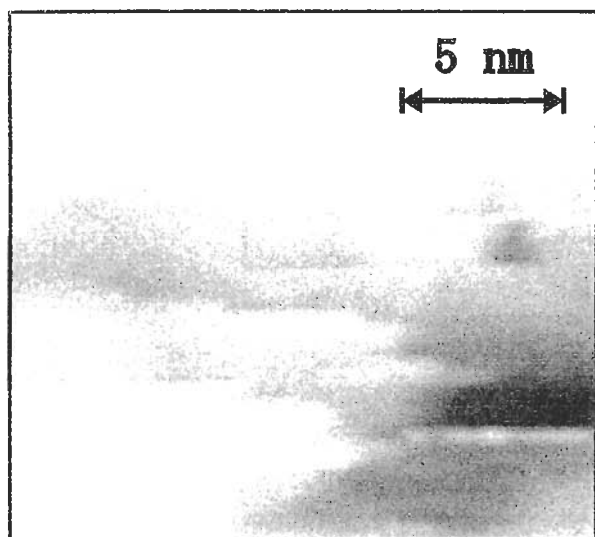
The samples and STM tips used to test the system were prepared as follows. For the purpose of studying photon emission from Au

surfaces, a Au film was evaporated onto the native oxide of a Si(001) sample under high vacuum conditions ( $10^{-5}$  Pa). In addition, two types of Si(001) samples were used for studying photon emission from dangling bonds on Si; an antimony doped ( $N_D = 1 \times 10^{18} \text{ cm}^{-3}$ ) sample and a boron doped ( $N_A = 1 \times 10^{18} \text{ cm}^{-3}$ ) sample. Si(001)-(3x1)-D surfaces were prepared by standard procedures<sup>16</sup>. These surfaces are constructed by an array of alternating dimerized monohydride rows and dihydride rows, where the monohydride rows consist of two dimerized Si atoms each bonded to a single D atom and the dihydride rows consist of single Si atoms each bonded to two D atoms<sup>16</sup>. If one of the D atoms is desorbed, a Si dangling bond appears and is observed as a bright spot in filled-state STM images. The 3x1 rather than the 2x1 reconstructed surface was chosen because the former was found to be more stable under high tunnel current and bias conditions of the STM as used in the photon emission experiments. Electrolytically

sharpened Au tips and tungsten (W) tips were employed in the experiments for the Au surfaces and the Si surfaces, respectively.

### 3. RESULTS AND DISCUSSIONS

Figure 3 shows (a) topographic image of a



(a)



(b)

Fig.3 Results of employing the PE-STM system to record a photon map of a Au surface, (a) STM topographic image of a Au surface using the scanning conditions  $V_b = -2$  V,  $I_t = 0.2$  nA and  $v_s = 27$  nm/s, and (b) the corresponding photon map recorded quasi-simultaneously with the topographic image.

Au surface using the scanning conditions  $V_b = -2$  V,  $I_t = 0.2$  nA and a scanning speed ( $v_s$ ) of 27 nm/s ( $t_{\text{pixel}} = 3.33$ ms) and (b) the corresponding



Fig.4 Results of employing the PE-STM system to record a photon map of a p-type Si(001)-(3x1)-D surface at negative sample bias, (a) STM topographic image before the photon emission experiment using  $V_b = -2$  V,  $I_t = 0.2$  nA and  $v_s = 1400$  nm/s, (b) STM topographic image using  $V_b = -3$  V,  $I_t = 8$  nA and  $v_s = 9$  nm/s and (c) photon map recorded quasi-simultaneously with (b).

photon map recorded quasi-simultaneously with the topographic image. The photon emission is expected to be due to radiative decay

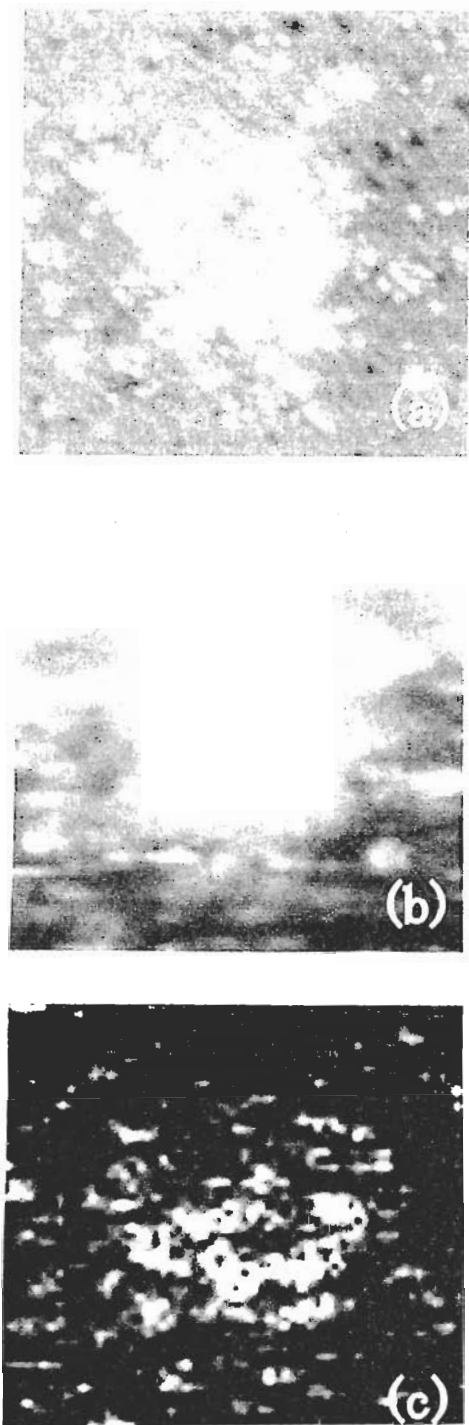


Fig.5 Results of employing the PE-STM system to record a photon map of a p-type Si(001)-(3x1)-D surface at positive sample bias, (a) STM topographic image before the photon emission experiment using  $V_b = -2$  V,  $I_t = 0.2$  nA and  $v_s = 1400$  nm/s, (b) STM topographic image recorded using  $V_b = +3$  V,  $I_t = 2$  nA and  $v_s = 9$  nm/s and (c) photon map recorded quasi-simultaneously with (b).

from localized surface plasmon modes<sup>13,17-20</sup>. The count rate for the brightest features in the frame [bright spot in the bottom part of Fig.3(b)] is  $\sim 1 \times 10^4$  CPS corresponding to a maximum quantum efficiency of  $\sim 2 \times 10^{-3}$ . This number agrees with the theoretical estimate for surface plasmons in small metal particles<sup>13</sup>. Note that there are correlations between the topographic image and the photon map [compare Figs.3(a) and (b)]. Some features are bright both in Fig.3(a) and in Fig.3(b), but other features appearing dark in the topographic image are bright in the photon map. This is most noticeably for the large bright spot in the bottom part of Fig.3(b). These observations agree with previous reports on photon emission from Au surfaces<sup>2,4,5,9,10,14,15</sup>.

Figure 4 shows the results of photon emission from an atomic scale pattern (10 nm x 10 nm) of dangling bonds (DBs) created by STM induced desorption of D atoms<sup>21</sup> on a p-type Si(001)-(3x1)-D surface. Fig.4(a) is a topographic image recorded before the photon emission experiment using  $V_b = -2$  V,  $I_t = 0.2$  nA and  $v_s = 1400$  nm/s, Fig.4(b) is a topographic image recorded using a negative  $V_b = -3$  V,  $I_t = 8$  nA and  $v_s = 9$  nm/s and Fig.4(c) is the photon map recorded quasi-simultaneously with (b). From the photon map, it is observed that the exposed DBs forming the square exhibit a large photon signal [ $\sim 160$  counts/second (CPS) in the bright regions in (b)], whilst the photon intensity from D terminated areas is much lower [ $\sim 27$  CPS].  $I_t$  was stable during recording the photon map excluding the possibility that the contrast in the photon map could be due to fluctuations in  $I_t$ . With the high voltage and current conditions during recording the photon map, the contrast of DB sites vs. D-terminated sites in Fig.4(b) almost disappears. However, there is a good contrast in the photon map [ see Fig. 4(c)]. In Fig.5, the corresponding results for the p-type sample are depicted for positive  $V_b$ , the scanning conditions in Fig.5(b) and (c) being  $V_b = +3$  V,  $I_t = 2$  nA and  $v_s = 9$  nm/s. The contrast in the photon map between DB sites and D terminated sites is 130/12. Similar to Fig.4(b), the contrast in the topographic image recorded at high current and voltage conditions is low [see Fig. 5(b)], but there is a good contrast in the photon map [see Fig.5(c)].

Results for the n-type sample are shown in Fig.6 for the case of negative  $V_b$  with (a) topographic image before the photon emission

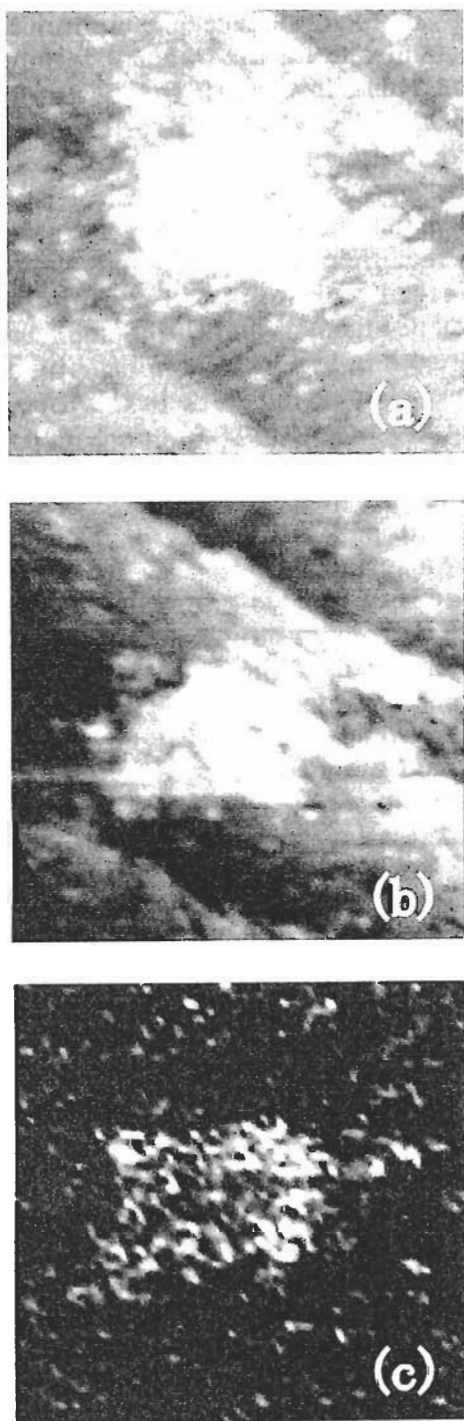


Fig.6 Results of employing the PE-STM system to record a photon map of an n-type Si(001)-(3x1)-D surface at negative sample bias, (a) STM topographic image before the photon emission experiment using  $V_b = -2$  V,  $I_t = 0.2$  nA and  $v_s = 1400$  nm/s, (b) STM topographic image recorded using  $V_b = -3$  V,  $I_t = 8$  nA and  $v_s = 9$  nm/s and (c) photon map recorded quasi-simultaneously with (b).

experiment using  $V_b = -2$  V,  $I_t = 0.2$  nA and  $v_s = 1400$  nm/s, (b) topographic image recorded using  $V_b = -3$  V,  $I_t = 8$  nA and  $v_s = 9$  nm/s and (c)

the photon map recorded quasi-simultaneously with (b). The contrast between DB sites and D terminated sites is 136/12. In the case of the n-type sample, we could not obtain any contrast in the photon map at positive  $V_b$ . This is presumably due to a strong band bending occurring for n-type Si(001) surfaces at positive sample biases<sup>22</sup>, which implies that large  $V_b$  and  $I_t$  are needed to get an acceptable photon intensity signal, but this will also result in an unacceptably high D desorption rate<sup>12</sup>.

In Fig.7 the photon intensity is plotted as function of  $I_t$  for  $V_b = +4$  V and  $V_b = -4$  V and for (a) the n-type sample and (b) the p-type sample. In these measurements, a band pass filter at 500 nm and a band width of 40 nm was positioned in front of the PMT. It is observed that the photon intensity increases almost linearly with increasing  $I_t$ . The quantum efficiency (QE) is estimated to be  $\sim 10^{-6}$ . Compared to gold, the photon signal from DBs on Si(001) surfaces is 3 orders of magnitude lower. The results therefore show that with the present system, we are able to obtain photon emission spectra and photon maps from

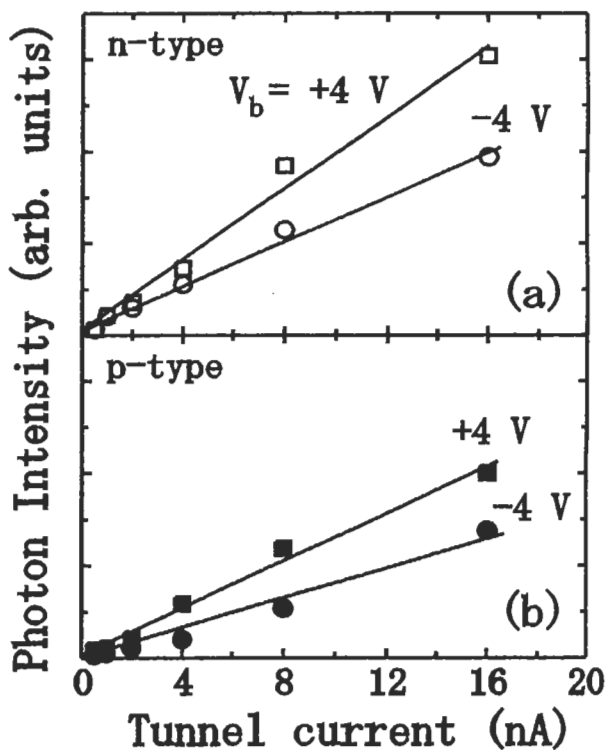


Fig.7 STM induced photon intensity from DB sites on Si(001)-(3x1)-D surfaces at  $\lambda = 500$  nm as function of  $I_t$  for a) the n-type sample and b) the p-type sample with  $V_b = -4$  V (circular symbols) and  $V_b = +4$  V (square symbols). The solid lines are linear fits to the data.

structures with aQE much lower than from metal surfaces<sup>2,4,5,9,10,14,15</sup>.

#### 4. Conclusions

A photon emission scanning tunneling microscope operating in UHV at room temperature has been reported. An optical fiber bunch with constant optical transmission from 400 nm to 1100 nm, a numerical aperture of 0.56 and a diameter of 1 mm was employed to collect the photons emitted from the tip of the STM. The optical fiber bunch is readily positioned close to the tip-sample region of the STM using an xyz-manipulator to obtain a good collection efficiency of the photons. With the present system the collection efficiency is ~4.5%, but this can be improved using fibers with a higher numerical aperture. The system exhibits a low number of undesirable photon counts from the stainless steel walls and the ion-pump in the UHV-chamber. Examples of photon emission from Au surfaces and dangling bond patterns on Si(001)-(3x1) D terminated surfaces were reported. It was shown that photon maps with good contrasts could be obtained with the present PE-STM from atomic scale structures with a quantum efficiency as low as  $\sim 10^{-6}$ .

#### References

1. J.K. Gimzewski, B. Reihl, J.H. Coombs, and R.R. Schlittler. *Z. Phys. Condensed Matter* **72**, 497 (1988).
2. R. Berndt, R. Gaisch, J.K. Gimzewski, B. Reihl, R.R. Schlittler, W.D. Schneider, and M. Tschudy, *Science* **262**, 1425 (1993).
3. R. Berndt, R.R. Schlitter and J.K. Gimzewski, *J. Vac. Sci. Technol. B* **9** 573 (1991).
4. R. Berndt, R. Gaisch, W.D. Schneider, J.K. Gimzewski, B. Reihl, R.R. Schlittler, and M. Tschudy, *Surf. Sci.* **307-309** 1033 (1994).
5. V. Sivel, R. Coratger, F. Ajustron, and J. Beauvillain, *Phys. Rev. B* **45** 8634 (1992).
6. S. Ushioda, *Solid State Commun.* **84** 173 (1992).
7. Ph. Dumas, M. Gu, C. Syrykh, A. Hallimaoui, and F. Salvan, *J. Vac. Sci. Technol. B* **12** 2064 (1994).
8. S. F. Alvarado, W. Ries, and P. F. Seidler, *Phys. Rev. B* **56** 1269 (1997).
9. K. Takeuchi, Y. Uehara, S. Ushioda, and S. Morita, *J. Vac. Sci. Technol. B* **9** 557 (1991).
10. M.J. Gallagher, S. Howells, L. Yi, T. Chen, and D. Sarid, *Surf. Sci.* **278**, 270 (1992).
11. T. Murashita and M. Tanimoto, *Jpn. J. Appl. Phys.* **34** 4398 (1995).
12. C. Thirstrup, M. Sakurai, and M. Aono, to be published.
13. Persson, B.N.J. and Baratoff, A. *Phys. Rev. Lett.* **68** 3224 (1992).
14. S. Ushioda, Y. Uehara and M. Kuwahara, *Appl. Surf. Sci.* **60/61** 448 (1992).
15. K. Ito, S. Ohyama, Y. Uehara, and S. Ushioda, *Surf. Sci.* **324** 282 (1995).
16. J.J. Boland, *Phys. Rev. Lett.*, **26**, 3325 (1990).
17. J.H. Coombs, J.K. Gimzewski, B. Reihl, J.K. Sass, and R.R. Schlitter, *J. Microsc.* **152** 325 (1988).
18. Johansson, P., Monreal, R. and Appel, P. *Phys. Rev. B* **42** 9210 (1990).
19. T. Schimizu, K. Kobayashi, and M. Tsukada, *Surf. Sci.* **60/61** 454 (1992).
20. Y. Uehara, Y. Kimura, S. Ushioda, K. Takeuchi, *Jpn. J. Appl. Phys.* **31** 2465 (1992).
21. Ph. Avouris, R.E. Walkup, A.R. Rossi, T.-C. Shen, G.C. Abeln, J.R. Tucker, and J.W. Lyding, *Chem. Phys. Lett.*, **257**, 148 (1996).
22. M. McEllistrem, G. Haase, D. Chen, and R.J. Hamers, *Phys. Rev. Lett.*, **70**, 2471 (1993).